Research on an Innovative FLEX Bicycle Frame with a Softtail Vibration Damping System

Łukasz Kuczek[1*], Paweł Marczak[2], Wacław Muzykiewicz[1], Marcin Mroczkowski[1], Paweł Paćko[3], Dawid Drop[4]

[1] AGH University of Science and Technology, Faculty of Non-Ferrous Metals, Aleja Adama Mickiewicza 30, 30-059 Kraków, Poland
[2] Loop LLC, Aleja 29 Listopada 130, 31-406 Kraków, Poland
[3] AGH University of Science and Technology, Faculty of Mechanical Engineering and Robotics, Aleja Adama Mickiewicza 30, 30-059 Kraków, Poland
[4] AG Motors LLC, Debica, Podgrodzie 34B, 39-200 Podgrodzie, Poland
* Corresponding author's email: lukasz.kuczek@agh.edu.pl

ABSTRACT

Bicycles are gaining inreasing popularity, especially in crowded cities where there is a problem with traffic jams and a limited number of parking spaces. The bicycles are also often used by mountain bikers during riding on off-road trails. In both cases, the important parameters of a bicycle design are the stiffness of the bicycle frame, the weight of the bicycle, but also driving comfort. To improve comfort and reduce vibrations in the bicycle frame both front and rear shock absorbers are used. The use of traditional shock absorbers increase the weight of the bike and its price. The work characterizes a modern Softtail damping system, designed by AG Motors. The spring-damping element was placed directly in the rear fork. Analyses of polyurethanes of various hardness levels were carried out in terms of the possibility of using them as a vibration damper. A numerical and experimental analysis of the bicycle frame were performed. Strength, fatigue and impact tests were carried out in accordance with the relevant bicycle standards. Research has shown that the frame bicycle with the Softtail system, meets the requirements of the standards and can serve as an effective equivalent of bikes equipped with the full suspension system.

Keywords: FLEX bike frame, Softtail damping system, elastomer, strength analysis, fatigue analysis, impact test.

INTRODUCTION

Bicycles are increasingly used as an everyday means of transport. It is estimated that there are over a billion bicycles in the world, and about 50% of the world's population can ride them. In many cities, more and more bicycle paths are created, both in the centres and on the roads leading to them. This allows for safe and relatively quick movement, especially in crowded urban areas. In recent years, interregional and international bicycle routes have been created, e.g. Green Velo Eastern Bicycle Trail or EuroVelo 10. Literature research shows that an appropriate bicycle infrastructure promotes driving comfort and promotes cycling [1, 2]. Cycling can also have a positive effect on human health and well-being, as well as improving the air quality [3]. However, one must not forget about the comfort of riding a bicycle, which, apart from reducing the weight of the bicycle and increasing the stiffness of the frame, is one of the important factors when designing bicycle frames [4]. The driving comfort is influenced, among other factors, by the vibrations the rider feels while riding. In [5] it was found that one of the important factors influencing the comfort of riding is the appropriate selection of the bicycle to the user, both in terms of height and the appropriate components of the bicycle. Another way to improve driving comfort is to use front

and/or rear shock absorbers. Their operation is based on the fact that they allow for additional non-simultaneous movement of the wheels in the vertical direction, thus dissipating terrain-induced energy [6, 7]. They contribute to the reduction of the feeling of impacts and vibrations transmitted to the frame and the rider. The use of a shock absorber can contribute to the reduction of physical stress, which is especially important during long journeys, but also during recreational riding [8]. The type of shock absorber, or rather the damping element, also affects the reduction of vibrations in the bicycle frame.

Appropriate design of a bicycle frame should include meeting the requirements, both in terms of strength and utility. This is especially important when designing bicycles for professionals and for special applications. For more recreational cyclists, the price and look have greater influence on the willingness to buy a bike [9]. Hence, bicycle frames are designed an optimized differently for a given target group. It is important that the bicycle frame is characterized by adequate stiffness, also when shock absorbers are used [10]. The stiffness and strength of the frame affect the manoeuvrability, precision of driving and comfort of cycling [11]. They depend, inter alia, on the structure of the frame itself [12–16], its material [17–20] or the shape of the tubes [21]. In the case of bicycles with a shock absorber, an additional important factor is the appropriate position of the shock absorber fastening element, so as to eliminate the smallest energy losses during riding due to the presence of a vibration damper [22]. At the stage of designing bicycle frames, computer modelling is often used [20,23,24], which allows to shorten the design process, as well as reduce its costs. Bicycles, as well as its individual elements, are also subjected to experimental tests aimed at, inter alia, determining how the designed element will behave under conditions similar to real loads [25–28]. ISO standard tests are also used to verify the design intent for the frame [29]. Hence, the process of designing a bicycle or its individual elements (including, in particular, a bicycle frame) is a long-term process that requires taking into account many factors and variables.

In the literature related to the subject of cycling, the greatest emphasis is placed on the optimization of the frame structure in terms of its usability. There is little research related to the analysis of the bicycle frame, especially with the innovative Softtail system (passive system), in terms

of meeting the requirements specified by bicycle standards. The paper presents the results of selected tests, both numerical and experimental, aimed at checking whether the newly designed FLEX frame structure, adapted to the use of the Softtail system, meets, inter alia, the requirements of international ISO standards in terms of its use for city and trekking bikes. The study also analysed the shock absorbing element (elastomer) used in the Softtail system in order to determine the minimum hardness of polyurethane.

Novel solutions for the construction of the vibration damping element in the bicycle frame

One of the most popular solutions of the shock absorbing system is the one-hinge or four-hinge suspension system. Another common system is the Monolink with three pivot points. However, the disadvantage of this type of solutions is the high complexity of the structure, and thus, higher weight, manufacturing and service costs. Hence, among bicycle manufacturers, other solutions for the construction of vibration damping elements in the bicycle frame are sought. One of the methods presented by Levy and Smith in [30] is the use of elastomer instead of pneumatic elements. A good vibration damping efficiency of the elastomer has been found. The Trek company, in the 1999 MTB bike, proposed to change the position of the rear shock absorber. Instead of attaching it directly to the seat tube, they mounted a muffler in the rear fork (Fig. 1). The most distinctive feature of the frame is the SilkTi Down Tube. This is a fully triangulated Ti6Al4V tall plate, known to engineers as a flat truss. The shock absorbing system uses an elastomer instead of a coil spring to improve the progressiveness of the damper. Thanks to this treatment, the weight was significantly reduced and the sensitivity of the shock absorption effect on small unevenness was improved.

A similar solution was used by BMC on a Teamelite bike equipped with the Micro Travel Technology (MTT) system (Fig. 2). Unlike the MTB solution, it is the most common solution in bicycle frames. In this case, the vibration damping element is made of elastomer. The system uses two hard anodized pins that thread into the seat stays through a pair of bushings. The frame, on the other hand, is entirely made of carbon composite. The flexibility of the rear fork of a bicycle frame is shaped by the arrangement of the

Fig. 1. 1999 MTB bike by Trek company (source: https://ibiscycles.
consumedesign.com/products/bikes/mtb/silk_ti/technology/)

fibre itself. The maximum deflection in this type of solution is about 15 mm.

FLEX frame structure with Softtail system

A new shock absorber solution related to the use of an elastomer as a vibration damping element was examined in this work (Fig. 3, red element). The main difference from other solutions of this type (e.g. Trek Supercaliber, BMC MTT) is the method of stiffening the system and fixing the elastomer. In the case of the BMC, pins are used that act as a guide for the movement of the seat stay. The FLEX frame with Softtail system, on the other hand, has the guiding cam that defines the movement of the seat stay. The advantage of this solution is the greater rigidity of the system and its life.

In this case FLEX frame witch Softtail system, the shock absorbing element is an elastomer made of polyurethane. The elastomer is mounted in specially designed casings. In order to avoid the possibility of falling out, the elastomer is screwed to the frame with two bolts, one for each housing. This allows the rear triangle to move freely in the vertical direction by compressing and expanding the elastomer while driving. By using elastomers of different hardness, it is possible to adjust the absorbing system to the user's requirements. The frame itself has a standard diamond shape, most
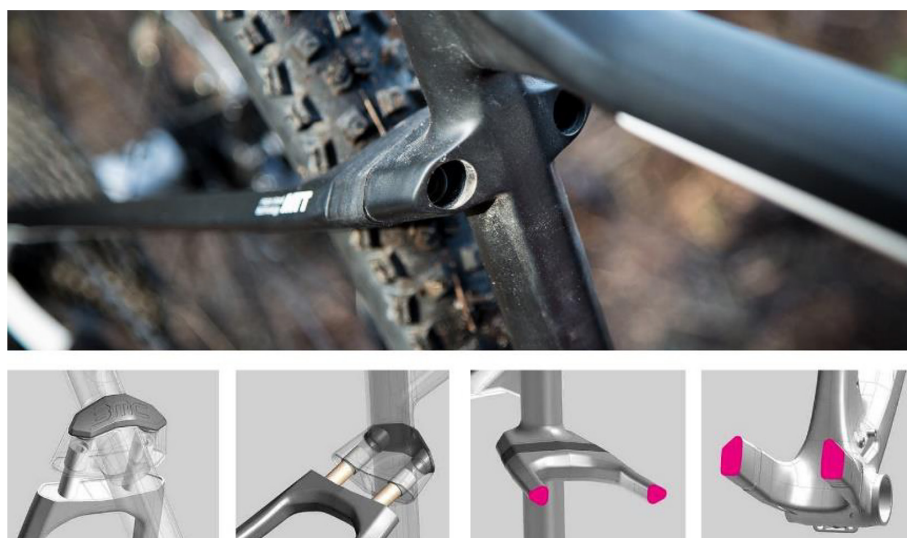

Fig. 2. BMC MTT system (source: https://bermstyle.com/
bmc-teamelite-29-hardtail-featureing-micro-travel-technology/)

Fig. 3. FLEX bicycle frame with Softtail system

commonly used in bicycle construction. At the same time, the fork is connected to the seat tube by means of a movable cam mounted on bearings. This allows the full use of the elastic properties of the elastomer and chainstey tubes.

The tubes intended for the individual elements of the bicycle frame are extruded and then shaped by hydroforming method. They are connected by GMAW welding. The resulting frame is then aged at 205°C for 1.5 hours. This is a standard method used in the production of bicycle frames by AG Motors LLC. The cam, on the other hand, is obtained by die casting. Polyurethane elastomer is obtained in two stages. First, the isocyanate is mixed with the polyol in the right proportions and then they are cast into the mold. The use of additional elements in the form of a cam (together with the instrumentation) and an elastomer makes the cost of such a frame higher by about 15% compared to a rigid bicycle frame. At the same time, comparing it to bicycle frames with typical dampers, the cost of the FLEX frame with the Softtail system is about 65% lower.

Research methodology and material

The work concerns a bicycle frame with a new bicycle suspension solution. It is a solution based on the Softtail system, in which the damping element is an elastomer made of polyurethane. The material of the metal elements of the bicycle frame (apart from the cam) was the 6061 T6 aluminium alloy with the chemical composition given in Table 1. Thermophysical and mechanical properties are shown in Tables 2 and 3, respectively. This alloy is one of the most commonly used materials in the construction of bicycle frames. This is due to, among other things, its good formability, good strength and stiffness-to-density ratio and good machinability [18,31]. In this type of alloys, it is also possible to carry out additional heat treatment of the frame after welding in order to increase its overall strength [32,33] and improve the quality of the joint [34–36]. Elastomers of different hardness (from 40 to 80 ShA), made of polyurethane, were used as the shock absorbing element. The material of the cam was WE43 magnesium alloy in the T6 state with the composition given in Table 1 and the properties shown in Tables 2 and 3. The cam was connected to the frame by plain bearings.

Numerical and experimental tests were carried out on the essential elements of the bicycle frame and the elastomer. Fatigue, endurance and impact tests (of falling mass) of the bicycle frame, both numerical and experimental, were performed. In the case of the shock absorbing element, it was subjected to numerical and experimental analysis in a compression test. Simulations were carried out for elastomers of different hardness. The geometry of the elastomer component is shown in the Figure 4. Assuming that the frame geometry only allows for compression or elastic stretching of the component along a predetermined axis (tangent to the movement of the component's anchor point in the swinging arm), an elastomer component compression test was performed. The displacement of the steel casing

Table 1. The chemical composition of the materials used in the FLEX bicycle frame

6061									
Al	Mg	Si	Cu	Fe	Mn	Cr	Ti	Zn	Rest
97.3	1.07	1.03	0.22	0.14	0.05	0.11	0.04	0.014	0.026
Mg WE43									
Mg	Y	Zr	Rare earth metals						
Rest	3.82	0.30	3.12						

Table 2. Physical and thermal properties of FLEX bicycle frame materials

Material	Density, g/cm³	Melting point, °C	Thermal conductivity, W/(m×K)	Specific heat capacity, J/(g×°C)	CTE, linear at 20 °C, μm/(m×°C)
Al 6061 T6	2.70	582–652	167.0	0.896	23.6
Mg WE43	1.84	545–640	51.3	1.00	26.0

Table 3. Mechanical properties of FLEX bicycle frame materials

Material	E, GPa	$R_{p0.2}$ [MPa]	R_m [MPa]	A_{10mm} [%]	HV
Al 6061 T6	69	258	291	10	100
Mg WE43		160	250	2	96

relative to the fixed base was 10 mm, which corresponds to the deformation of the elastic element of about 25%. A standard tetragonal mesh with an average element size of approximately 2 mm was used. Based on numerical analyses, a numerical model of the elastomer equivalent element was built and used during computer simulations of the FLEX bicycle frame with the Softtail system. The equivalent (linear) stiffness of the elastomer was identified based on a virtual compression test of the element shown in Figure 4. For both materials used in the study, i.e. steel and rubber (elastomer), linear constitutive relations were used with the respective parameters of Young's moduli and Poisson ratios reported in the following section. The nonlinear Green-Lagrange strain tensor and a geometric-nonlinear solution procedure were adopted in the simulation. Adaptive incremental stepping strategy was employed, first using the multiplicative-updated Langrangian approach,

followed by the additive updated Lagrangian strategy in case of convergence failure. The full Netwon-Raphson solution technique with relative residual force testing with 10% error allowed was adopted. The equivalent linear stiffness was extracted from the least squares linear fit to the force-displacement characteristics acquired in the simulation.

An experimental elastomer compression test was carried out on a testing machine with simultaneous measurement of the force and displacement of the traverse (Fig. 5). In order to perform the compression test, an appropriate fixture simulating the casing elements in the frame was constructed. The cross-section of the elastomers affected by the applied force was approximately 82.4 cm². The initial height of the tested elastomers in the active range was 30 mm. Five compression-unloading cycles were performed for each elastomer.

The deformation of the test specimens was in each case about 50%, which corresponded to a displacement of the traverse of 15 mm. The compression test was carried out with three different speeds of the traverse: 5, 10, 15 mm/min.

For the entire bicycle frame (including the elastomer), a simulation of normative tests were carried out according to the conditions contained in the ISO 4210–6 standard. The numerical calculations of the bicycle frame were carried out in the MSC.Marc FEA software with all elements described by the linear stress-strain relation (or linear force-displacement relation for the elastomeric element). The solution procedure adopted for the frame analysis was the same as for the virtual compression test of the elastomer described earlier. For this purpose, a virtual model of the frame geometry was prepared as a mainly surface object (Fig. 6a). Only in the case of the muff and the elements holding the equivalent elastomer element
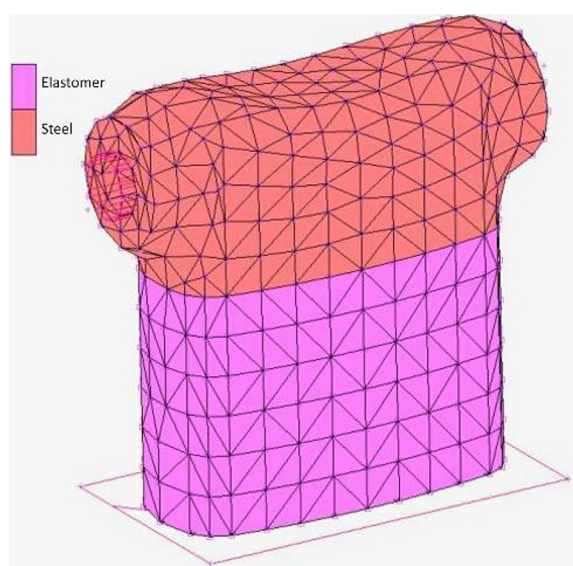

Fig. 4. Numerical model with tetrahedral mesh of elastomer in a steel casing
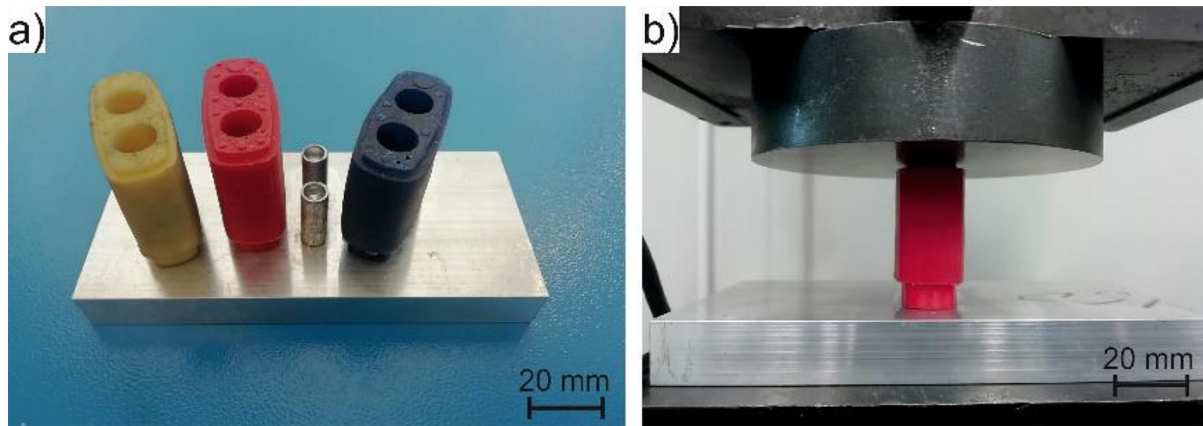
Fig. 5. Elastomers of different hardness (a) and elastomer compression (b)

(linear spring) and the cams, solid objects were used. The Figure 6b shows the thickness distribution of the elements in the frame used during the analyses, together with the rigid and substitute elements. Properties of the materials used in the calculations are presented in Table 4. In numerical studies, a four-noded quadrilateral elements were used for shell regions and a tetrahedral mesh element for solid elements. The average size of the mesh was approximately 0.5 mm. The value of the force and the method of loading of the frame were selected according to ISO 4210–6 standard. Chain, crank and pedal components were assumed to be massless and rigid.

The frame of the FLEX bicycle with the innovative Softtail system has been subjected to experimental tests, in which strength, fatigue and impact tests were carried out. During the tests, deformations and stresses were measured at six selected measurement points of the frame. For this purpose, resistance strain gauges were glued to the bicycle frame and connected in half-bridge systems. The places where the sensors are attached are marked as in Figure 7a. The active strain gauges were glued axially both on the upper (marking "u") and bottom (marking "d") surfaces of the tubular elements that make up the bicycle frames. For each place marked in the Figure 7a, strain gauges were glued in two areas at the top and bottom of the tube. Figure 7b shows an example of gluing strain gauges in the place marked as 2. Compensation strain gauges were glued to separate plates that were not deformed. In the tests the TFs-10 strain gauges ($R = 350.5$ Ω $k = 2.19$) were used. Measurements were made using the Spider 8 device with six strain gauge measuring channels. The research was carried out in the research facility of AG Motors (Fig. 7c).
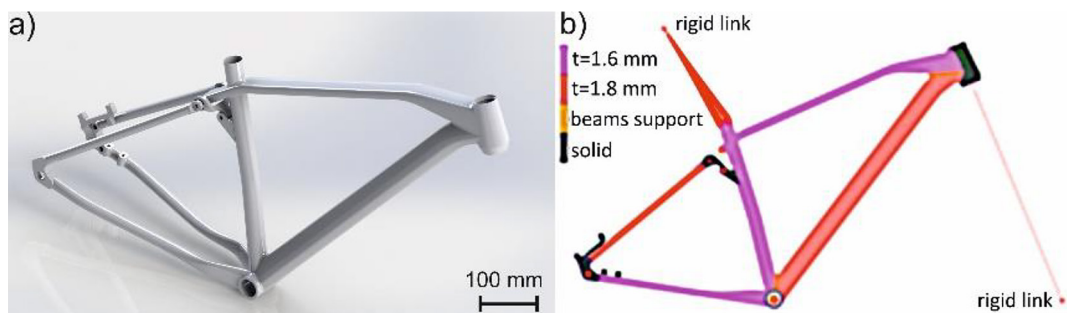

Fig. 6. Virtual model of the bicycle frame (a) and the thickness distribution in the bicycle frame (b)

Table 4. Basic properties of materials used in numerical analysis

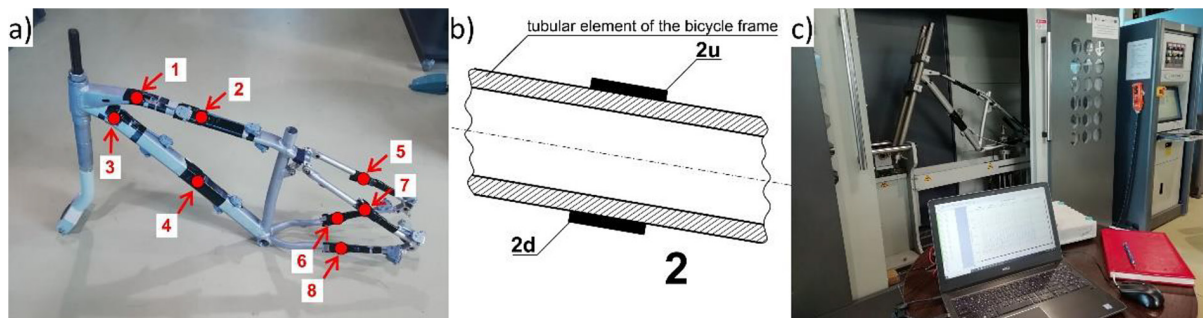| Material	Aluminium 6061 T6	Mg WE43-T6
Young modulus	70 000 MPa	44 200 MPa
Poisson's ratio	0.33	0.27
Density	2700 kg/m³	1840 kg/m³

Fig. 7. The way of sticking the strain gauges (a), method of gluing strain gauges (b) and the test stand (c)

RESULTS AND DISCUSSION

Damping element for the bicycle frame with the Softtail system

One of the essential components of the Softtail solution is the elastomer (spring-damping element). It serves as a vibration damper during cycling, both in urban and more demanding conditions – during mountain riding. Its functionality is significantly influenced by the hardness of the material from which it is made.

Figure 8 shows exemplary compression diagrams for elastomers of different hardness. In all cases, a differences in the character of the curves were found for the compression and relaxation stages. With the increase in polyurethane hardness, the compressive force $F_{50\%}$, necessary to deform the damping element by 50% of its height, also increased (Fig. 9a). For an elastomer with a hardness of 40 ShA, its value was about 185 N, while for the damping element with the highest hardness (80 ShA), the force was over 1400 N. These values correspond to the load with a mass of 19 kg and 145 kg, respectively. The analysis shows that an elastomer with a hardness of 40 ShA
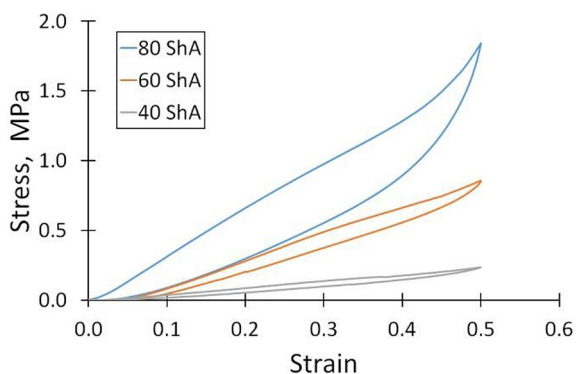

Fig. 8. Exemplary relations between stress and deformation of samples for full ranges of elastomers loads for compression speed of 15 mm/min

and lower cannot be used as a vibration damper due to too low forces it can transmit and too low stiffness of frame. The compression speed also influenced the value of the $F_{50\%}$ force (Fig. 9b). As the speed of the traverse movement increased, the force $F_{50\%}$ also increased. In the case of the elastomer with a hardness of 80 ShA, for which the influence of velocity was the greatest, the increase in the force value was about 100 N, while for the soft polyurethane (40 ShA) the difference was only 13 N.

When determining the hardness of polyurethanes of different hardness, it was found that there is an approximate relationship between the penetration depth of the indenter and the hardness, and between the penetration depth and the pressure force. These dependencies were assumed to be linear within a limited range of deformations (40–80 ShA). This allowed to determine the relationship between the Young's modulus E of the elastomer and its Shore hardness:

$$E = \frac{1 - v^2}{2RC_3} \cdot \frac{C_1 + C_2 A}{100 - A} \qquad (1)$$

where: n – Poisson's ratio of the elastomer (0.49), R, C_1, C_2, C_3 – constants, A – Shore hardness; $R = 0.395$, $C_1 = 0.549$, $C_2 = 0.07516$, $C_3 = 0.025$.

In the tested range of elastomer hardness (from 40 to 80 ShA), the values of the polyurethane longitudinal elasticity modulus increased curvilinear with hardness, reaching the value of about 13 MPa for a material with a hardness of 80 ShA (Fig. 10).

As part of the analysis of the behaviour of the damping element under compressive load, a simulation of compression of an elastomer with a selected stiffness together with a casing element was also carried out. The highest deformation of the component was found for the free part of the elastomer (Fig. 11a), which was confirmed by
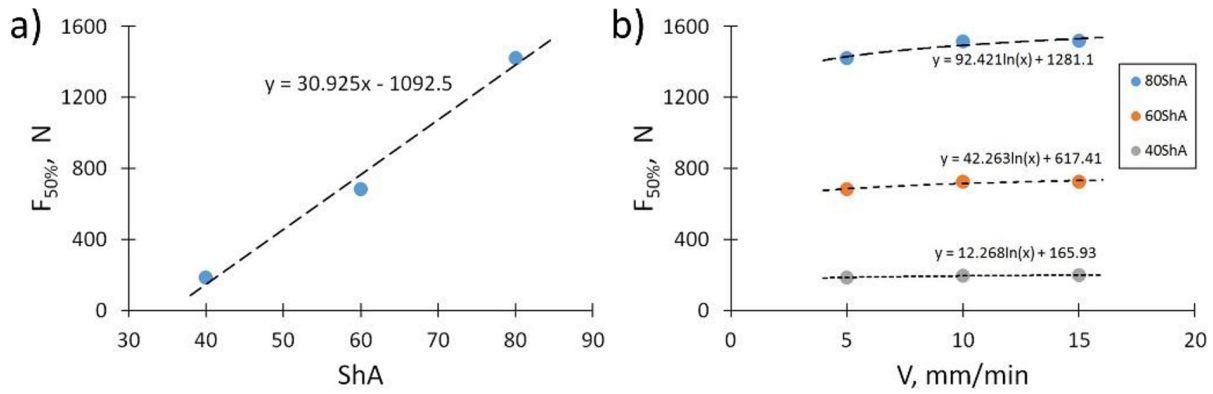
Fig. 9. The influence of elastomer hardness (a) and compression speed (b) on the value of the force $F_{50\%}$

the results obtained during the experiment under similar load (Fig. 11b). The highest stresses were recorded at the location of the elastomer clamp, below the bearing bore. At this point, on the one hand, there is the bearing's pressure on polyurethane. On the other hand, the casing limits the elastomer's ability to freely deform at this point. Hence, additional compressive stresses appear as a reaction of the elastomer pressing against the walls of the clamp. Their values, however, are so low that they do not adversely affect the operation

of the entire system. The stresses in the deformed area of the elastomer do not exceed the level of 4 MPa (for the deformation equal to 25%).

Based on the obtained results of the simulation of elastomer compression, an equivalent numerical model of the shock absorbing element was constructed, for which an equivalent stiffness linear coefficient of 100 N/mm was assumed. This model was used during further numerical analysis of the bicycle frame.
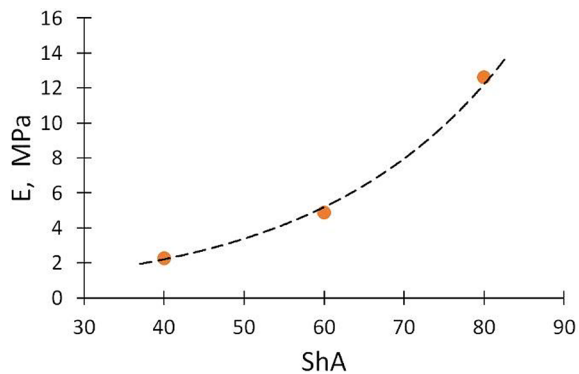
FLEX frame with an innovative Softtail system

An important element of the bicycle frame test is the analysis of its structure in terms of its behaviour under various loads and compliance with the requirements included, among others, in ISO 4210–2 and ISO 4210–6. These tests allow for the verification of design assumptions and the elimination of errors that may have occurred during the design of the frame.

In the case of fatigue tests, the requirement for the bicycle frame to meet the standards is the absence of visible cracks and fractures in the frame. The tests confirmed the fulfilment of
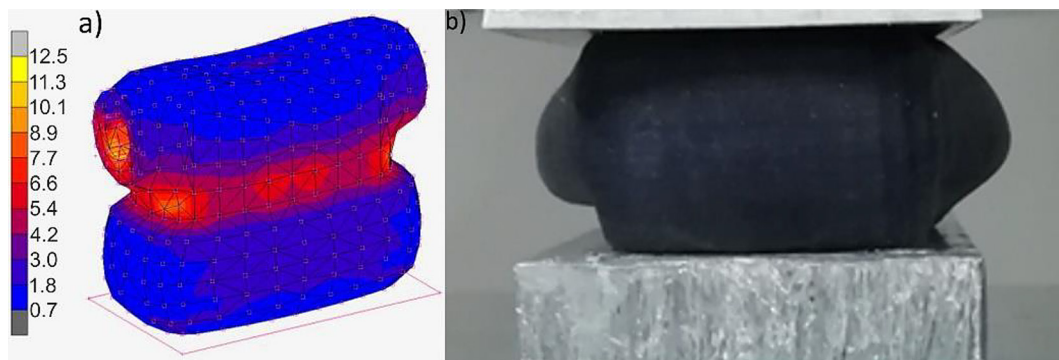

Fig. 10. Dependence of Young's modulus on elastomer hardness

Fig. 11. Equivalent von Mises stress distribution in an elastomer with a hardness of 80 ShA (a) and appearance of the elastomer under compressive load (b)

these requirements. Both in the case of loading the frame with a force applied in the horizontal and vertical direction, there was no damage to the frame. Based on the computer simulations carried out, it was found that in the case of a load with a horizontal force of the front fork, the area with the highest stress value is the place where the tubes of the front triangle of the frame connect to the head of the frame (Fig. 12), especially when applying a force in the direction of travel (tensile force). However, there were no areas where the permissible stresses for the material were exceeded. The highest value of equivalent stresses in the structure, recorded after 100 000 cycles, did not exceed the value of 110 MPa. For the load directed against the direction of travel, the highest loads were found in the area of bending of the lower tubes of the rear forks (Fig. 13).

The performed strain gauge tests confirm the results obtained during the numerical analysis. When loading the front fork with a variable horizontal force, the greatest deformations were found in the case of the front tube of the frame (Fig. 14a), in the bend area of the down tube, near the point of connection with the head tube. The strain at this point was 0.141% (Fig. 14b), which corresponded to a tensile stress of about 99 MPa.

The rear forks of the frame, in which the shock absorbing element was placed, were not significantly deformed (Figs. 14c and 14d). The slight difference in deformation (0.002%) is due to the slightly different shape of the chainstay tubes.

The use of an elastomeric shock absorber, mounted in the rear fork near the seat tube, contributed to greater front fork displacement. Compared to the stiff Mustang frame (without rear shock absorber), the front fork displacement of the FLEX Softtail frame was higher, regardless of the direction of force (Fig. 15). Compared to a rigid frame, the Softtail frame has a greater ability to dampen vibrations.

When loaded with a vertical force applied to the saddle, the nature of the stress distribution in the frame also changes (Fig. 16). Its highest values appeared at the junction of the top tube and the seat tube. This is due to the way the test is carried out in which the front and rear forks are fixed. This causes accumulation of stress in the frame at the point where the triangles (front and rear) connect at the seat tube. At this point, the bending moments in the frame in this test also reach their highest values. It should be noted that in the actual test, the load is distributed over the greater length of the seat tube with the help of
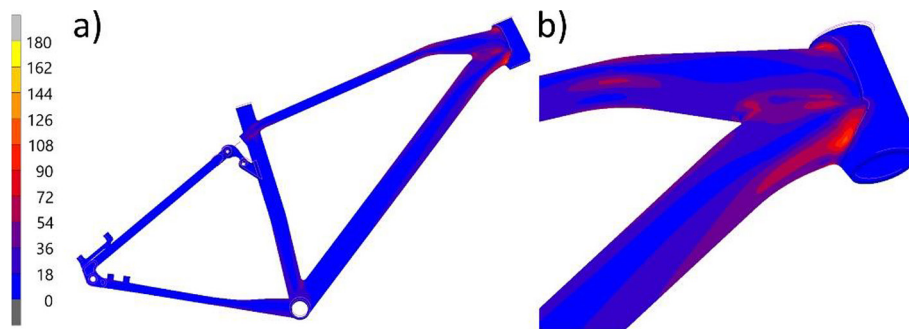

Fig. 12. Equivalent von Mises stress distribution in the bicycle frame during the fatigue test (load applied in the direction of travel of the bicycle): full view (a), head tube (b)
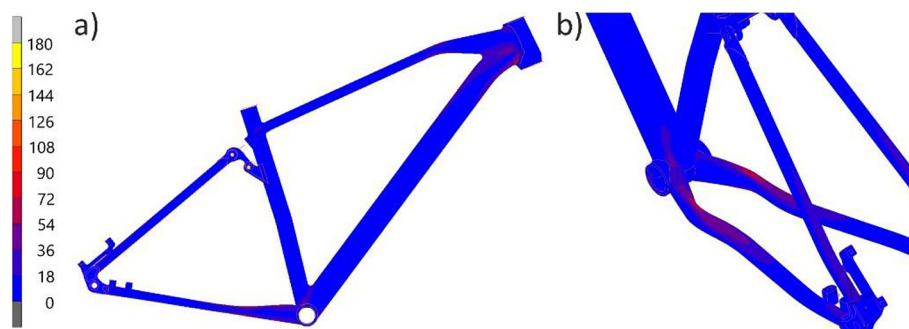

Fig. 13. Equivalent von Mises stress distribution in the bicycle frame during the fatigue test (load applied against the direction of travel of the bicycle): full view (a), bicycle muff (b)

the seat post. The maximum stress values in this area did not exceed the yield strength of the frame material (aluminium alloy 6061 T6).

The results of the numerical analysis were confirmed by a strain gauge test. As in the simulation, in the area of the upper and lower tube of the front triangle, the stress values did not exceed 35 MPa (Fig. 17). Higher stresses were found at the measurement site in the lower tubes of the chainstays (maximum 45 MPa). This was due to the design of these elements and the use of smaller diameter tubes, which had to transfer about 60% of the pressure applied to the seat tube. An important area is also the place where the forks connect to the muff (Fig. 16). For front triangle contact, the location of the stress practically goes where the down tube passes into the seat tube. In the remaining area, the stresses do not exceed 30 MPa. On the other hand, rigidly connecting the frame's rear fork to the lower part of the seat tube and to the upper part by means of a movable element in the form of a vibration damping system, increases the stress in the chainstays. This increase includes not only the connection with the seat tube and muff, but also the areas of inflection resulting from the presence of a wide bicycle tire in this place. High values of equivalent stress are

mainly located on the surface of the upper and lower tubes (Fig. 16), while on the side surfaces its values do not exceed 20 MPa. This is due to the presence of high compressive and tensile stresses in this area during the test, which are a consequence of bending the pipes at this point. As shown by simulations and strain gauge tests, the stresses are much lower in the remaining areas of the rear fork. This means that in addition to the connection of the top tube of the frame with the seat tube, the critical points of the construction of the bicycle frame, especially with the Softtail system, are also the areas where the lower tubes of the rear forks are connected to the muffle.

Drop-mass impact test is a destructive test. As a result, the frame is permanently damaged, caused by the impact of a hammer of appropriate energy (about 40 J). For frames intended for MTB and city bikes, the standard allows the maximum permanent deformation of the frame, resulting from the impact, equal to 10 mm. In this test, the most vulnerable areas of the frame are mainly the front triangle top and bottom tubes. The results of the computer simulation of the test show that in the case of the tested FLEX frame with the Softtail system, the highest stress values occur at the point of connection
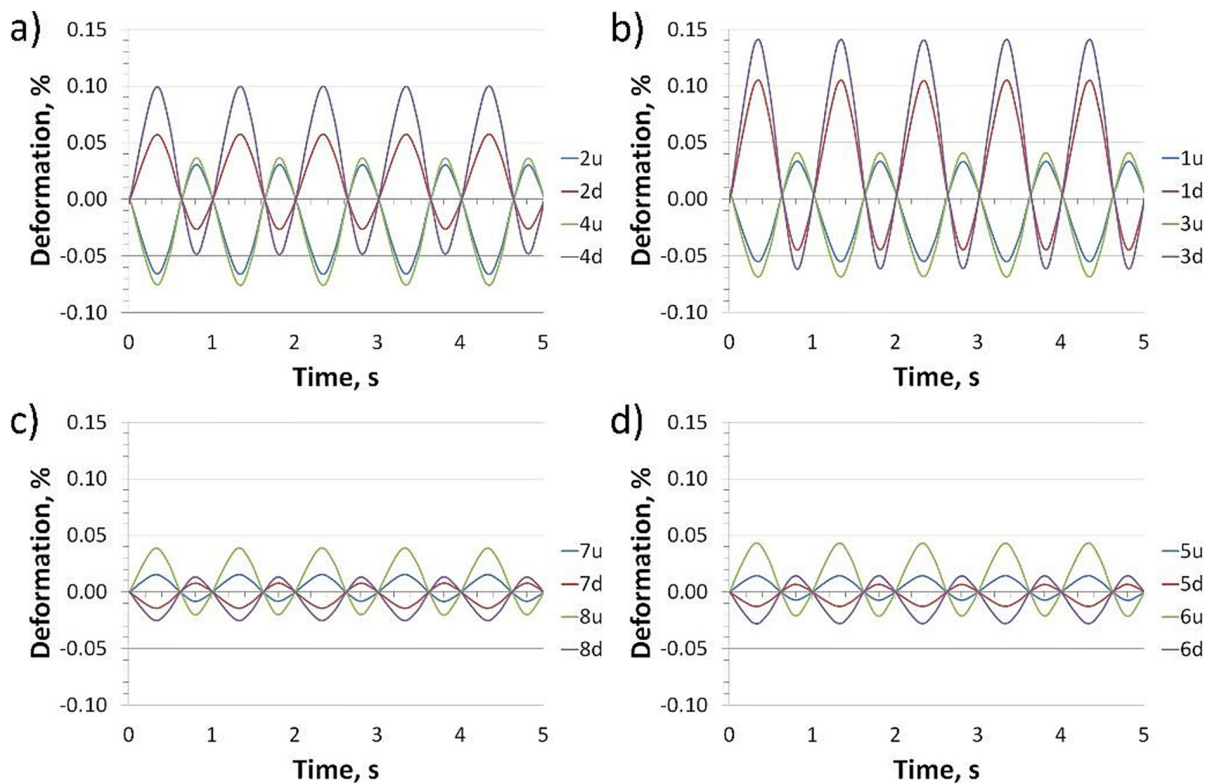

Fig. 14. Experimental results of the deformation of front tube (a), head tube (b), left (c) and right (d) rear triangle, obtained with a vertical load on the bicycle frame
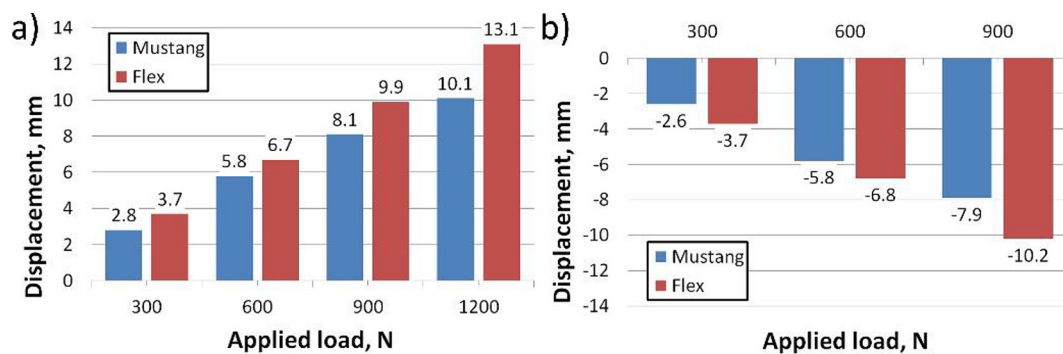
Fig. 15. Front fork displacement in FLEX and Mustang frames depending on the applied load

of the pipes with the head tube and on the bend of the upper tube of the front triangle (Fig. 16). This is mainly due to the fact that in this area, the greatest absorption of the energy of the falling hammer by the frame takes place. Stress values in excess of the tensile strength of the material were also found in the weld area of the downtube and head. This means that there is a high probability of cracks appearing at this point. The increase in the value of the equivalent stress also appears in the places where the front triangle of the frame joins the seat tube. However, unlike the head tube area, its values at these locations do not exceed the yield strength of 6061 T6 alloy. Experimental studies confirmed the simulation results. The frame was subjected to permanent deformation, as a result of which the hammer travelled a distance (from the moment of contact with the head of the frame to its stop) equal to approximately 5 mm, which did not exceed the maximum shortening value. The strain values, measured with strain gauges placed in the test areas, exceeded the limit value of 0.2% (Table 5). The greatest strain of -0.302% was recorded at the point 3, i.e. in the bend of the front lower tube of the bicycle frame from the bottom. The pipe has been permanently bent at this point.

The frame during the impact of the impactor was characterized by a relatively high stiffness. The falling mass, at the moment of impact, bounced off the frame and fell again. The change of the deformation value with time was of a damped harmonic character (Fig. 19). After unloading, the permanent deformation of the frame in the place of its greatest strain was at the level of 0.1%.

CONCLUSIONS

The paper presents an analysis of a FLEX bicycle frame with a Softtail shock absorbing system. It is a system that allows for good damping of rear wheel vibrations by deflecting the rear forks up to about 30 mm vertically. The appropriate selection of the elastomer material allows for an individual approach to the user's requirements in terms of the hardness of the compressed element. Research has shown that the use of polyurethane with too low hardness causes that the designed system does not fulfil its role as the dumper. Based on the results, it can be concluded that the hardness of the elastomer should not be less than 60ShA. In the case of more extreme conditions of using a bicycle with the Softtail system,
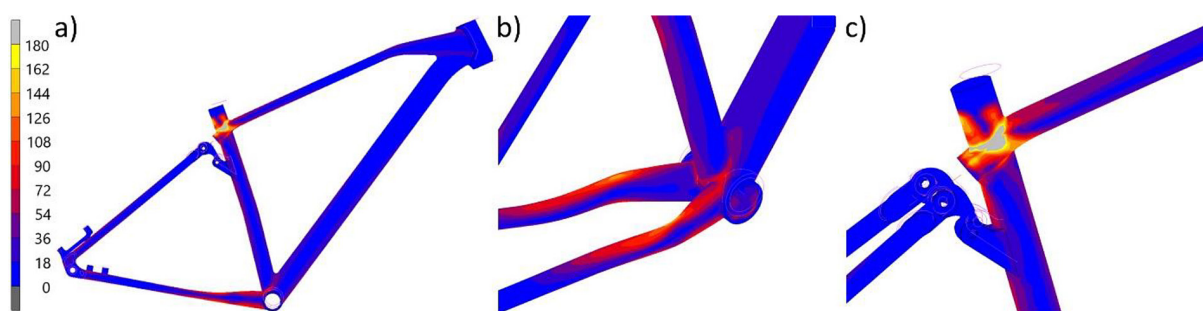

Fig. 16. Equivalent von Mises stress distribution in the bicycle frame during the fatigue test (vertical load applied to the seat): full view (a), bicycle muff (b), top of the seat tube (c)
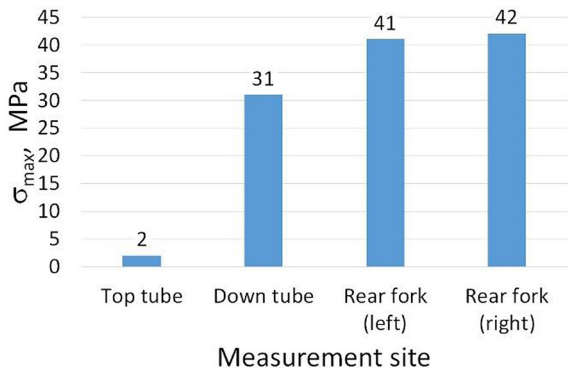
Fig. 17. Maximum stresses in selected places of the bicycle frame

the hardness of the damping element should be even higher (at least 80 ShA). The deformation of such an elastomer requires the application of

almost twice as much force as in the case of an element with a hardness of 60 ShA.

An important step in the design of bicycle frames and new solutions related to, for example, the vibration damping system, is the need to check the frame in terms of its strength, resistance to fatigue and impact resistance. Regardless of the tests performed, both numerical and experimental analyses have shown that the designed FLEX frame with the Softtail system meets the requirements set out in the relevant bicycle ISO standards. The frame is characterized by good strength and resistance to the effects of applied cyclic forces (horizontal to the front fork, vertical to the seat tube). The critical points of the tested frame are especially the connections of the tubes: the upper tube with the seat tube, the front triangle
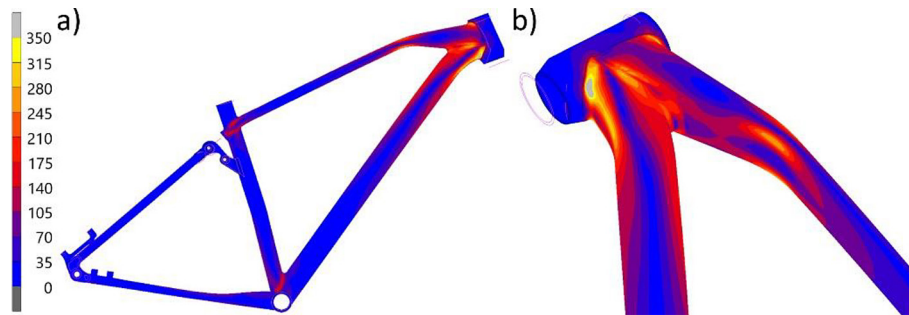

Fig. 18. The stress distribution in the bicycle frame during the impact test: full view (a), head tube (b)

Table 5. The greatest strains at selected points of the Flex bicycle frame during impact

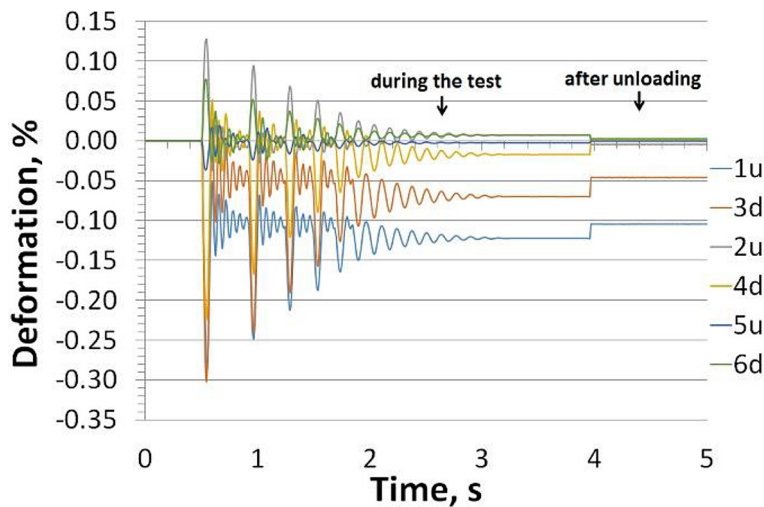| Stress type	Strain, %					
	1d	3d	2u	4d	5u	6d
Tensile	0,000	0,027	0,128	0,051	0,019	0,077
Compressive	-0,290*	-0,302*	-0,037	-0,224*	-0,037	-0,028

Fig. 19. Deformations during impact and after the Flex frame is relieved

tubes with the head tube and the lower tubes of the chainstay with the socket. Stress locations of greater or lover value appear in these areas, depending on where the load is applied. However, only in the destructive test they were so large that they contributed to damage to the frame. Nevertheless, the tested frame with the Softtail system still met the requirements of the standard for city and trekking bikes.

Further research is planned on the FLEX bicycle frame with the Softtail system. We plan to conduct other tests, both numerical and laboratory, included in the ISO 4210–2 and ISO 4210–6 standards. In addition, measurements of stresses in the frame during cycling in real conditions are planned.

Acknowledgments

REFERENCES

1. Hunt J.D., Abraham J.E. Influences on bicycle use. Transportation. 2007; 25;34(4): 453–470.

2. Martens K. Promoting bike-and-ride: The Dutch experience. Transportation Research Part A: Policy and Practice. 2007; 41(4): 326–338.

3. Gupta M.R. Analysis of Mountain Bike Frame By F.E.M. IOSR Journal of Mechanical and Civil Engineering. 2016; 13(2): 60–71.

4. Vanwalleghem J., Mortier F., De Baere I., Loccufier M., Van Paepegem W. Design of an instrumented bicycle for the evaluation of bicycle dynamics and its relation with the cyclist's comfort. Procedia Engineering. 2012 ;34: 485–490.

5. Christiaans H.H.C.M., Bremner A. Comfort on bicycles and the validity of a commercial bicycle fitting system. Applied Ergonomics. 1998; 29(3): 201–211.

6. Needle S.A., Hull M.L. An Off-Road Bicycle With Adjustable Suspension Kinematics. Journal of Mechanical Design. 1997; 1;119(3): 370–375.

7. De Lorenzo D.S., Hull M.L. Quantification of Structural Loading During Off-Road Cycling. Journal of Biomechanical Engineering. 1999; 1;121(4): 399–405.

8. Nielens H., Lejeune T. Bicycle Shock Absorption Systems and Energy Expended by the Cyclist: Sports Medicine. 2004; 34(2): 71–80.

9. Hsiao S.W., Ko Y.C. A study on bicycle appearance preference by using FCE and FAHP. International Journal of Industrial Ergonomics. 2013; 43(4): 264–273.

10. Wu C.C., Ballance D. Static and free vibration analyses of a bike using finite element method. International Journal of Engineering Research. 2015; 1(7): 60–86.

11. Ferraresi C., Garibaldi L., Perocchio D., Piombo B.A.D. Dynamic behavior and optimization of frames for road and mountain bikes. In San Jose, CA, United States; 1998.

12. Wang J.H., Zhao J.N., Zhao Y.S., Wang Z., Guo D.L. Simulation about Sports Bicycle Frame Based on the Experiments. AMM. 2010; 37–38: 1142–1147.

13. Covill D., Begg S., Elton E., Milne M., Morris R., Katz T. Parametric Finite Element Analysis of Bicycle Frame Geometries. Procedia Engineering. 2014; 72: 441–446.

14. Lin C.C., Huang S.J., Liu C.C. Structural analysis and optimization of bicycle frame designs. Advances in Mechanical Engineering. 2017; 9(12): 168781401773951.

15. Devaiah B.B., Purohit R., Rana R.S., Parashar V. Stress Analysis of A Bicycle Frame. Materials Today: Proceedings. 2018; 5(9): 18920–18926.

16. Akhyar, Husaini, Iskandar H., Ahmad F. Structural Simulations of Bicycle Frame Behaviour under Various Load Conditions. MSF. 2019; 961: 137–147.

17. Davis R., Hull M.L. Design of Aluminum Bicycle Frames. Journal of Mechanical Design. 1981; 1; 103(4): 901–907.

18. Rontescu C., Cicic D.T., Amza C.G., Chivu O.R., Dobrota D. Choosing the optimum material for making a bicycle frame. Metalurgija -Sisak then Zagreb. 2015; 54(4): 679–682.

19. Suyitno, Salim U.A. Fabrication of Bicycle Frame of A356 Aluminum Alloys by Using Sand Casting. AMM. 2015; 758: 131–135.

20. Sarath P., Akash D., Hrishikesh H., Nimisha S.D., Jinuchandran. Stress Analysis of Bicycle Frame using Different Materials by FEA. GRD Journal for Engineering. 2021; 6(7): 14–20.

21. Covill D., Blayden A., Coren D., Begg S. Parametric Finite Element Analysis of Steel Bicycle Frames: The Influence of Tube Selection on Frame Stiffness. Procedia Engineering. 2015; 112: 34–39.

22. Karchin A., Hull M.L. Experimental Optimization of Pivot Point Height for Swing-Arm Type Rear Suspensions in Off-Road Bicycles. Journal of Biomechanical Engineering. 2002; 1; 124(1): 101–106.

23. Sani M.S.M., Nazri N.A., Zahari S.N., Abdullah N.A.Z., Priyandoko G. Dynamic Study of Bicycle Frame Structure. IOP Conf Ser: Mater Sci Eng.

2016; 160: 012009.

24. Khutal K., Kathiresan G., Ashok K., Simhachalam B., Davidson Jebaseelan D. Design Validation Methodology for Bicycle Frames Using Finite Element Analysis. Materials Today: Proceedings. 2020; 22: 1861–1869.

25. Arola D., Reinhall P.G., Jenkins M.G., Iverson S.C. An experimental analysis of a hybrid bicycle. Exp Techniques. 1999; 23(3): 21–24.

26. Champoux Y., Vittecoq P., Maltais P., Auger E., Gauthier B. Measuring the dynamic structural load of an off-road bicycle frame. Experimental Techniques. 2004; 28(3): 33–36.

27. Champoux Y., Richard S., Drouet J.M. Bicycle Structural Dynamics. Sound and Vibration. 2007; 41(7): 16–22.

28. Koellner A., Cameron C.J., Battley M.A. Measurement and Analysis System for Bicycle Field Test Studies. Procedia Engineering. 2014; 72: 350–355.

29. Cheng Y.C., Lee C.K., Tsai M.T. Multi-objective optimization of an on-road bicycle frame by uniform design and compromise programming. Advances in Mechanical Engineering. 2016; 1; 8(2): 168781401663298.

30. Levy M., Smith G.A. Effectiveness of vibration damping with bicycle suspension systems. Sports Eng. 2005; 8(2): 99–106.

31. Demir H., Gündüz S. The effects of aging on machinability of 6061 aluminium alloy. Materials & Design. 2009; 30(5): 1480–1483.

32. Ozturk F., Sisman A., Toros S., Kilic S., Picu R.C. Influence of aging treatment on mechanical properties of 6061 aluminum alloy. Materials and Design. 2010; 31: 972–975.

33. Rajaa S.M., Abdulhadi H.A., Jabur K.S., Mohammed G.R. Aging Time Effects on the Mechanical Properties of Al 6061-T6 Alloy. Eng Technol Appl Sci Res. 2018; 18; 8(4): 3113–3115.

34. Ahmad R., Bakar M.A. Effect of a post-weld heat treatment on the mechanical and microstructure properties of AA6061 joints welded by the gas metal arc welding cold metal transfer method. Materials and Design. 2011; 32: 5120–5126.

35. Perez JS, Ambriz RR, Lopez FFC, Vigueras DJ. Recovery of Mechanical Properties of a 6061-T6 Aluminum Weld by Heat Treatment After Welding. Metallurgical and Materials Transactions A. 2016; 47: 3412–3422.

36. Fadaeifard F., Matori K.A., Garavi F., Al-Falahi M., Sarrigani G.V. Effect of post weld heat treatment on microstructure and mechanical properties of gas tungsten arc welded AA6061-T6 alloy. Transactions of Nonferrous Metals Society of China. 2016; 26: 3102–3114.